

Intermittent suppressive posaconazole therapy is ineffective at mitigating cardiac and digestive tract pathologies in an experimental model of chronic Chagas disease

Shiromani Jayawardhana,¹ Francisco Olmo,^{1,2} Amanda Fortes Francisco,¹ Archie A. Khan,¹ Michael D. Lewis,¹ Martin C. Taylor,¹ John M. Kelly¹

AUTHOR AFFILIATIONS See affiliation list on p. 12.

ABSTRACT Infections with *Trypanosoma cruzi* cause Chagas disease, a chronic condition that can give rise to debilitating cardiac and/or gastrointestinal damage. However, it is unclear why only ~30% of individuals progress to symptomatic pathology, why this can take decades to become apparent, and why there is such a wide range of disease outcomes. Disease pathology is a long-term cumulative process resulting from collateral damage caused by inflammatory immune responses that continually eliminate transient parasite infections in the heart and/or gastrointestinal tract. The guiding principle behind anti-parasitic drug development is that a sterile cure is required to prevent progression to symptomatic pathology. Evidence suggests that the cumulative damage required to reach the symptomatic threshold is determined by a number of factors, including host and parasite genetics, which govern the intensity and location(s) of infection. Therefore, an alternative therapeutic strategy could involve long-term intermittent treatment, which may not confer sterile cure but is able to suppress the parasite burden to a level where the disease does not become symptomatic within the lifetime of the infected individual. To test this hypothesis, we used an experimental murine model that displays both cardiac and digestive tract pathologies. Mice were given intermittent treatment with posaconazole under conditions that initially reduced the parasite burden by >99% but did not confer sterile clearance. Our results show that this did not provide long-term protection against the key cardiac or gastrointestinal manifestations of Chagas disease, and that sterile cure should remain the single goal of the drug development community.

KEYWORDS Chagas disease, *Trypanosoma cruzi*, posaconazole, intermittent treatment, pathology

Chagas disease caused by the protozoan *Trypanosoma cruzi* poses a public health challenge across Latin America (1). In addition, due to migration, it is increasingly detected in non-endemic regions (2, 3). Parasite transmission occurs primarily via triatomine bug vectors, but other routes of infection, such as congenital transmission, consumption of contaminated food and drink, organ transplantation, and blood transfusions, also pose significant risk (4–7). Following *T. cruzi* infection, individuals enter the acute stage, which typically lasts 2–8 weeks and is characterized by widespread parasite dissemination in blood and tissues. Symptoms at this stage are usually mild or non-specific, although outcomes can be fatal in some cases due to myocarditis or encephalopathy. Immune responses eventually control, but do not eliminate the infection, and most individuals then remain asymptomatic for life (8–10). Approximately 30% of those infected ultimately develop chronic Chagas disease, although this can take decades to become symptomatic (11). *T. cruzi* infection results in chronic Chagas

Editor Audrey Odom John, The Children's Hospital of Philadelphia, Philadelphia, Pennsylvania, USA

Address correspondence to John M. Kelly, john.kelly@lshtm.ac.uk.

The authors declare no conflict of interest.

See the funding table on p. 12.

Received 29 November 2024

Accepted 2 April 2025

Published 5 May 2025

Copyright © 2025 Jayawardhana et al. This is an open-access article distributed under the terms of the [Creative Commons Attribution 4.0 International license](https://creativecommons.org/licenses/by/4.0/).

cardiomyopathy (CCC) in 20–30% of cases, and ~10% lead to digestive Chagas disease (DCD), with the symptoms sometimes occurring in combination (12–14).

Several mechanisms have been postulated to explain the underlying causes of CCC, including direct parasite-mediated injury, parasite-induced inflammatory tissue damage, and autoimmune responses (15–18). The most widely accepted view is that pathology results from cumulative damage to heart tissue caused by pro-inflammatory immune responses driven by the presence of parasites. This in turn leads to fibrosis, cardiac hypertrophy, and cardiomyopathy, although disease progression follows a complex pathway that can also involve arrhythmias and thromboembolisms and is difficult to predict at an individual level (10, 19–21). During chronic *T. cruzi* infection, the parasite burden is extremely low and can be challenging to detect in some patients. In murine models, the gastrointestinal (GI) tract, skin, and in some strains, skeletal muscle, act as permissive reservoirs where infection foci persist (22–25). Cardiac infections in the chronic stage appear to be periodic rather than persistent, with detectable infection ranging from 10 to 80% depending on the mouse-parasite strain combination. Persistent cardiac infection is not required for the development of fibrosis (22, 23). Rather, intermittent cardiac infection, perhaps a result of parasite trafficking from more immune-tolerant niches, seems to be sufficient. The resulting pro-inflammatory responses continually eliminate these periodic infections but often to the detriment of the surrounding tissue (19). Cardiac muscle and nervous tissue have low regenerative capacity, a feature that may explain the progressive nature of the pathology (26). The complex nature of Chagas disease has made it difficult to address the precise nature and progression of cardiac pathology in humans.

In the case of DCD, outcomes can include changes in motility, secretion, and absorption, particularly in the colon and esophagus (14, 27, 28). Irreversible denervation in the enteric nervous system has been proposed to lead to progressive dysfunction in gut motility involving difficulty in swallowing, slower GI transit, and feces retention, finally leading to megacolon or megaesophagus (29, 30). Recently, a murine model of DCD has been developed, in which a digestive transit delay and feces retention are associated with chronic *T. cruzi* persistence in the colon (31). This model provides a platform for dissection of DCD pathogenesis (32).

For several decades, *T. cruzi* infections have been treated with the nitroheterocyclic drugs benznidazole and nifurtimox (33, 34). Despite their long-standing use, there are several issues that contribute to a high level of treatment failure (10–50%) (35, 36). These include treatment duration (60–90 days), toxicity that leads to patient non-compliance, and variable efficacy across the *T. cruzi* species. In addition, both of these pro-drugs are bio-activated within the parasite by the same mitochondrial nitroreductase (TcNTR-1), which could lead to cross-resistance (37, 38). To address these challenges, there is an international effort driven by large drug-development consortia to extend the range of therapeutic options. A promising candidate that emerged early in this process was the anti-fungal drug posaconazole, an inhibitor of *T. cruzi* sterol 14 α -demethylase (CYP51), an enzyme involved in ergosterol biosynthesis (39, 40). Posaconazole exhibited *in vitro* antiparasitic activity in the low nanomolar range, displayed promising *in vivo* efficacy, had a good safety profile, and was already licensed for human use (41, 42). Unfortunately, it ultimately failed in clinical trials (35, 43), and more sensitive *in vivo* studies in mice revealed an inability to provide regular sterile cure (44).

There is abundant evidence from animal experiments that curative benznidazole treatment can block the development of cardiac pathology, particularly if delivered early in an infection (17, 45, 46). Similarly, in the case of murine DCD, curative treatment in the acute stage halts disease progression, reverses the gut motility defect, and leads to a recovery in the density of colonic myenteric neurons (31, 32). In contrast, although non-curative treatment results in initial improvement in GI tract symptoms, this is transient, with infection relapse leading to a return of pathology. Collectively, these experiments provide a strong rationale for the consensus that the presence of the

parasite is required to drive the immune-mediated tissue damage that results in Chagas disease pathology.

The target product profile for new Chagas disease drugs describes a candidate that provides parasitological cure during the asymptomatic chronic stage of the infection (47). This is in accordance with our current understanding of disease pathogenesis, which predicts that timely intervention should block further development of pathology (17, 32). The discovery of new drugs that conform to this profile has been demanding (48). Given the progressive nature of Chagas disease, an alternative treatment strategy could involve long-term intermittent administration of therapeutics that are able to reduce the parasite burden sufficiently to slow the acquisition of tissue damage, so that symptomatic pathology and organ dysfunction do not arise during the lifetime of the patient. To test this hypothesis, *T. cruzi*-infected mice were treated long-term with posaconazole under conditions in which the parasite burden was greatly reduced but not eliminated. The results strongly indicate that sterile cure is necessary to protect against the development of both cardiac and GI tract pathologies.

RESULTS

To determine if suppressive intermittent therapy could prevent or moderate the progression of Chagas disease pathology, posaconazole was selected because of its anti-parasitic profile (44) and low toxicity (41, 42). In addition, we had previously shown that this drug could reduce splenomegaly in mice chronically infected with *T. cruzi*, even when sterile cure was not achieved (44). We used female C3H/HeN mice infected with the bioluminescent *T. cruzi* JR-Luc strain (Materials and Methods). In this infection model, the acute stage parasite burden peaks 3–4 weeks post-infection (wpi) (23, 49), and mice develop chronic cardiac (17, 23, 50) and digestive (31, 32) pathologies.

The experimental outline is shown in Fig. 1. Beginning 21 days post-infection (dpi), mice were treated with posaconazole once daily for 12 days (20 mg/kg). By the end of this period, bioluminescence levels had been reduced by >99%, close to background levels (Fig. 2). One cohort of mice was given no further treatment (initial treatment group). The infection relapsed in all these mice, such that within 2–3 weeks of drug withdrawal, the parasite burden had returned to levels similar to those in non-treated control mice. There was then a reduction in parasite load, as the infection transitioned to the chronic stage (>11 wpi), with infection foci displaying a typically dynamic spatiotemporal profile (Fig. 2). After the initial treatment, a second cohort of mice was treated at monthly intervals (monthly treated group) for 5 days at 20 mg/kg until the experimental

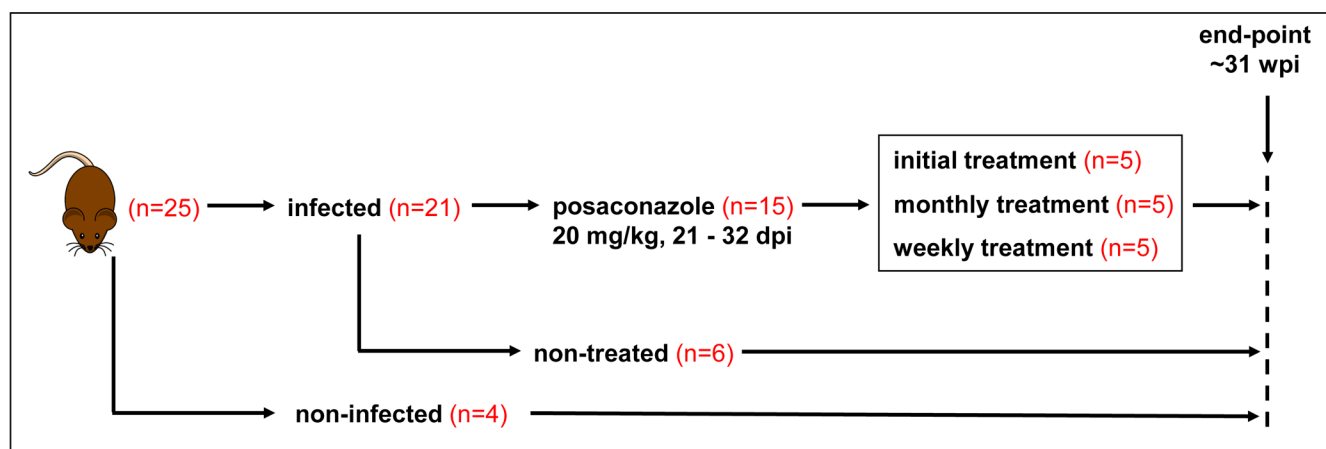


FIG 1 Experimental outline. C3H/HeN mice were infected with the bioluminescent *T. cruzi* JR-Luc strain (DTU I). At 21 days post-infection (dpi), they were treated once daily with 20 mg/kg posaconazole for 12 days (Materials and Methods). One cohort of mice was given no further treatment. A second cohort was treated with posaconazole (20 mg/kg) for 5 days each month, and a third was treated 1 day each week until the experimental end-point at 31 weeks post-infection (wpi). All mice were subjected to necropsy and analysis at this point.

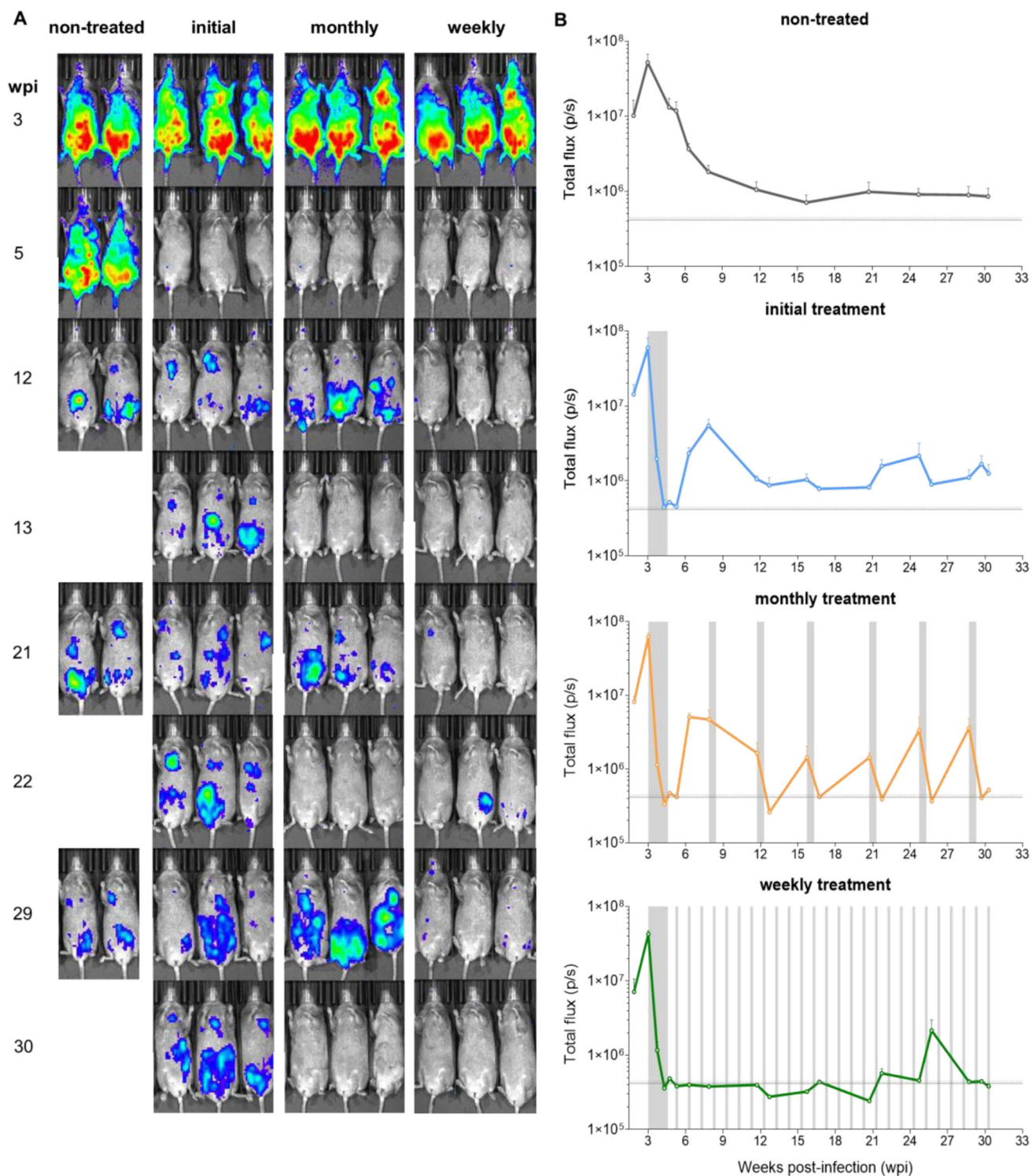


FIG 2 *In vivo* assessment of intermittent posaconazole treatment of *T. cruzi*-infected mice. (A) C3H/HeN mice were infected with the bioluminescent *T. cruzi* JR-Luc strain and monitored regularly by *in vivo* imaging (ventral images shown). As outlined (Fig. 1), 21 dpi, mice were treated with posaconazole (20 mg/kg) once per day for 12 days. After this initial dosing, one group ($n = 5$) received no further treatment (initial). A second group ($n = 5$) was subsequently treated on five consecutive days each month (monthly), and a third group ($n = 5$) was treated weekly with a single dose of 20 mg/kg posaconazole (weekly). The heat map is on a log₁₀ scale and indicates intensity of bioluminescence from low (blue) to high (red). (B) Graphs showing the total body bioluminescence (ventral and dorsal imaging) (photons/second; p/s) of treated and non-treated mice throughout the experiment. The gray vertical bars indicate treatment periods.

end-point (31 wpi). With each mouse, monthly treatment resulted in a reduction in bioluminescence-inferred parasite burden to background levels, followed by a relapse. There was a tendency for the rebound in parasite burden to increase with time, such that later in the experimental schedule, it peaked at levels higher than in non-treated control mice (Fig. 2). In the third cohort, after the initial treatment period, mice were treated weekly with a single 20 mg/kg dose (weekly treatment group). With this regimen, parasites were barely detectable by *in vivo* imaging until 22 wpi, and as with the monthly dosing cohort, the extent of relapse then tended to increase, although this was not consistent (Fig. 2).

All mice were examined by *ex vivo* imaging at the experimental end-point (Materials and Methods; Fig. 3). This confirmed that all mice in the treatment groups were still infected. Bioluminescent foci were detectable in the GI tract and skin in all cases, whereas in other organs and tissues, including the heart, infection was more sporadic. At the endpoint, the overall level of infection in mice that received only the initial 12-day dosing or received monthly intermittent treatment was similar to non-treated mice. Mice that received the single weekly dose had fewer detectable foci (Fig. 3), possibly reflecting that they had received their final posaconazole dose 3 days before the end-point at 31 wpi (Fig. 2). The limit of detection by *ex vivo* imaging is <12 parasites (24).

To determine if the trend of relapses becoming more pronounced over time was linked to acquired resistance (Fig. 2), 12 parasite clones were isolated from a range of mouse tissues (Materials and Methods). None of the clones displayed increased tolerance to posaconazole, as inferred from treatment of infected COLO-N680 cell cultures (Fig. S1).

All mice were assessed regularly throughout the experimental period for GI transit time delays as a marker for DCD after oral gavage with the red dye tracer carmine (Materials and Methods) (Fig. 4A, Fig. S2). As observed previously (31, 32), non-treated mice developed a delay during the acute stage, which peaked at 4.5 wpi. After partially subsiding, severity increased later in the chronic stage (24 wpi and beyond) (Fig. 4A). Non-curative posaconazole treatment (initial treatment group) led to a rapid reversal of the GI transit delay back to levels observed in the non-infected controls. However, the effect was temporary; the transit time reverted to that in non-treated mice by week 12, with severity increasing further by the experimental end-point (30 wpi). A detailed temporal breakdown and statistical analysis of the transit delay data are provided in Fig. S2. In the cohort of mice that were given additional monthly treatment, the reversal of the transit delay was maintained until beyond week 18, but then reached a level similar to that of non-treated mice by week 24 (Fig. 4A; Fig. S2). Treated mice given

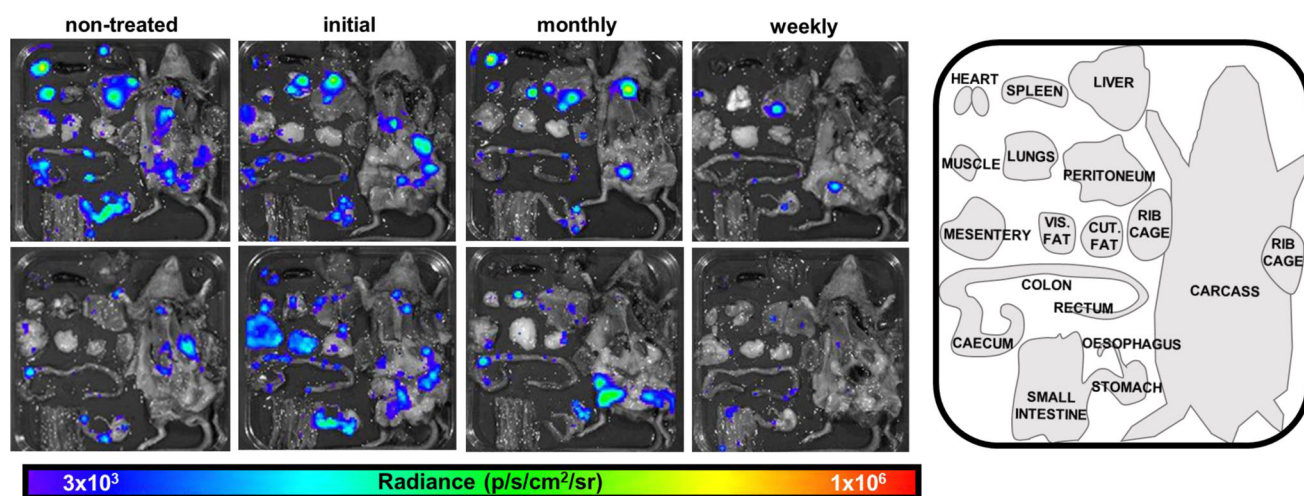


FIG 3 End-point tissue and organ distribution of *T. cruzi* following various posaconazole treatment regimens. Two representative *ex vivo* images of tissues and organs harvested from mice in each cohort at the experimental end-point (31 wpi) (Materials and Methods). Tissues/organs were arranged as shown (inset, right). The heat map is on a log₁₀ scale and indicates intensity of bioluminescence from low (blue) to high (red).

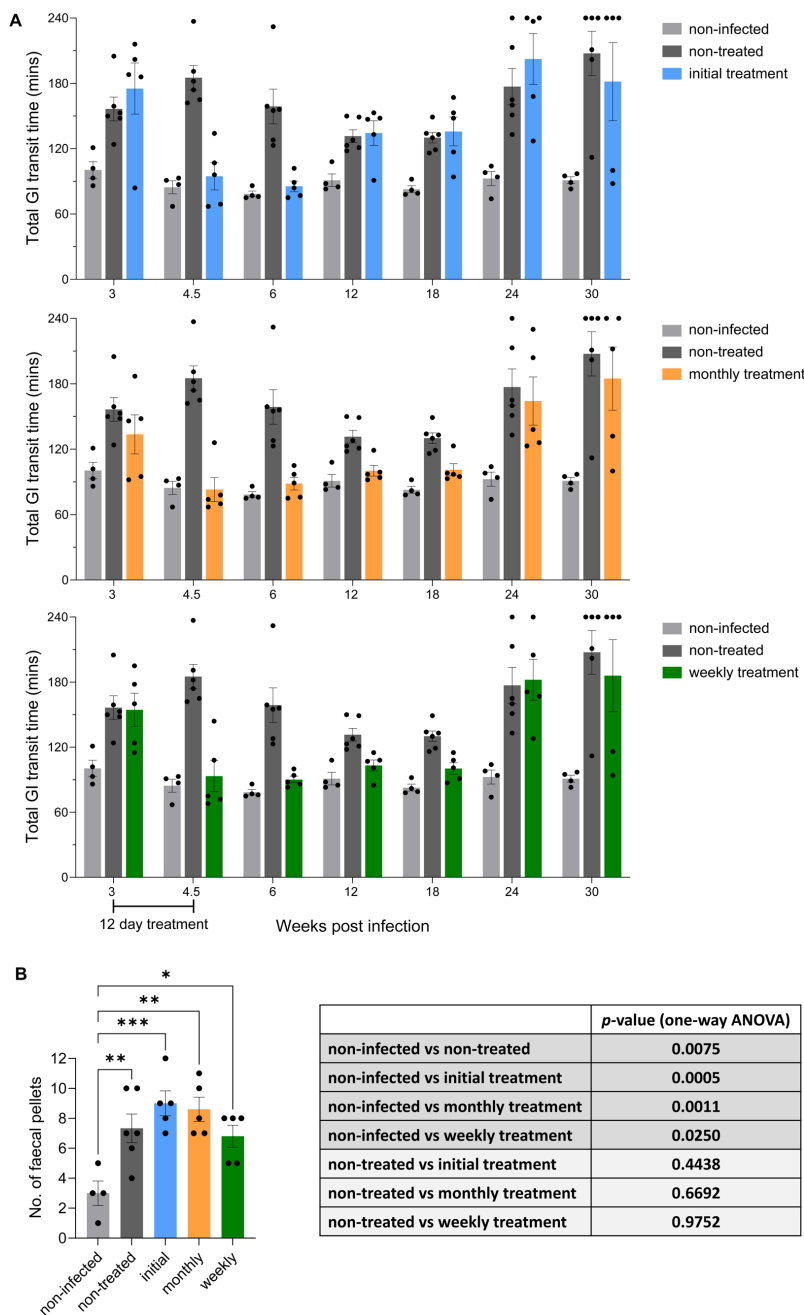


FIG 4 Intermittent posaconazole treatment does not protect *T. cruzi*-infected mice from GI tract dysfunction. (A) Bar charts showing the impact of posaconazole treatment on GI transit time in C3H/HeN mice infected with the *T. cruzi* JR-Luc strain (non-infected mice, $n = 4$; non-treated mice, $n = 6$; each treatment group, $n = 5$). Transit times were established by monitoring the passage of the red dye tracer carmine (Materials and Methods). A 4 h (240 min) cut-off point for transit data acquisition was imposed for animal welfare reasons. Each dot represents a single mouse. Data are expressed as mean \pm standard error of the mean (SEM). See Fig. S1 for details on statistical analysis. (B) Bar chart showing the number of fecal pellets in the colon *post-mortem* (Materials and Methods) of non-infected mice, infected non-treated mice, and infected mice treated with posaconazole (initial, monthly, and weekly), as outlined in Fig. 1 and 2. Each dot represents a single mouse, with data expressed as mean \pm SEM. Asterisks represent P -values for one-way analysis of variance, followed by Dunnett's multiple comparison *post-hoc* test (* $P < 0.05$; ** $P < 0.01$; *** $P < 0.001$). All infected groups showed a significant difference to the non-infected group. There was no significant difference ($P > 0.05$) between any of the treated groups and the non-treated group, as shown in the table.

weekly doses of posaconazole followed the same trend. At 30 wpi, several mice from all infected groups displayed transit time delays beyond the 4 h cut-off period, implying the development of severe chronic DCD pathology (Fig. 4A).

At the experimental end-point, we also investigated the impact of the treatment regimens on the development of a constipation phenotype (31, 32) by assessing retention of fecal pellets in the colon after 2 h fasting. Pellet numbers in each of the treated cohorts were found to be more than twice those in colons from non-infected mice (Fig. 4B) and not statistically different from mice that were non-treated. In this infection model, we previously observed that non-curative benznidazole treatment during the acute stage leads to a transient improvement in GI tract motility and function (32), but during the chronic stage, the extent of pathology reverts to that in non-treated mice. Our results here show that this chronic stage outcome also occurs, even when suppressive intermittent treatment is administered at weekly or monthly intervals for the duration of the infection.

To evaluate the ability of suppressive posaconazole treatment to block the development of cardiac pathology, quantitative analysis of collagen content was used as an indicator of pathological myocardial fibrosis (Materials and Methods). In non-infected age-matched control mice, the collagen content was notably consistent (15 cardiac images examined per mouse) (Fig. 5), and three to four times lower ($P = 0.01$) than in non-treated infected mice. There was greater variation in the levels of fibrosis in infected mice, an observation that has been made previously (17) and which reflects the situation found in human infections. No significant difference in collagen content was observed between non-treated mice and those from the initial treatment group. Similarly, in the infected mice exposed to the weekly or monthly posaconazole treatment regimens, the extent of collagen deposition was not significantly different from the non-treated cohort, with no apparent benefit arising from the intermittent regimen.

DISCUSSION

Drug development strategies against *T. cruzi* infections are based on a perceived need to achieve sterile cure (47). An alternative strategy could be the long-term use of drugs, which might not eliminate the infection but is able to maintain the parasite burden below a threshold required to drive symptomatic pathology during the lifetime of the infected individual. A crucial requirement of such drugs would be an acceptable safety profile under long-term use, for example, similar to that of statins. To test this hypothesis, we selected posaconazole, a well-tolerated anti-fungal drug (41, 42) that reduces *T. cruzi* infections to very low levels but typically does not eliminate the parasite (35, 43, 44). The initial treatment conditions (20 mg/kg for 12 days) reduced the parasite burden below the level of detection by *in vivo* imaging but was followed by relapse in all cases (Fig. 2 and 3). Monthly treatment resulted in the parasite burden being temporarily reduced to background levels, only for it to rebound, sometimes higher than in the non-treated control mice, when drug pressure was released (Fig. 2). Despite these relapses, the continued ability of treatment to knock down the parasite load suggested that long-term intermittent dosing did not result in the development of posaconazole resistance. This was confirmed by assessing the posaconazole sensitivity of parasites rescued from infected mice at the experimental end-point (Fig. S1). Posaconazole is considered to be a trypanostatic drug, and activity against intracellular parasites *in vitro* reaches a plateau where increasing drug concentration no longer results in further growth inhibition (51). With *T. cruzi* JR-Luc, intracellular growth inhibition of the isolated parasite clones plateaued between 65 and 75% at all concentrations tested between 8 and 500 nM (Fig. S1). Increases in the extent of recrudescence after multiple suppressive treatments (Fig. 2A) might, therefore, reflect a selective bottleneck that allows parasites with a slightly higher *in vivo* growth rate to dominate the population.

DCD is an enteric neuropathy that in the C3H/HeN:TcJR-Luc host:parasite model results in a GI transit delay that first becomes apparent during the acute stage of infection (32). This is then followed by partial recovery before further deterioration

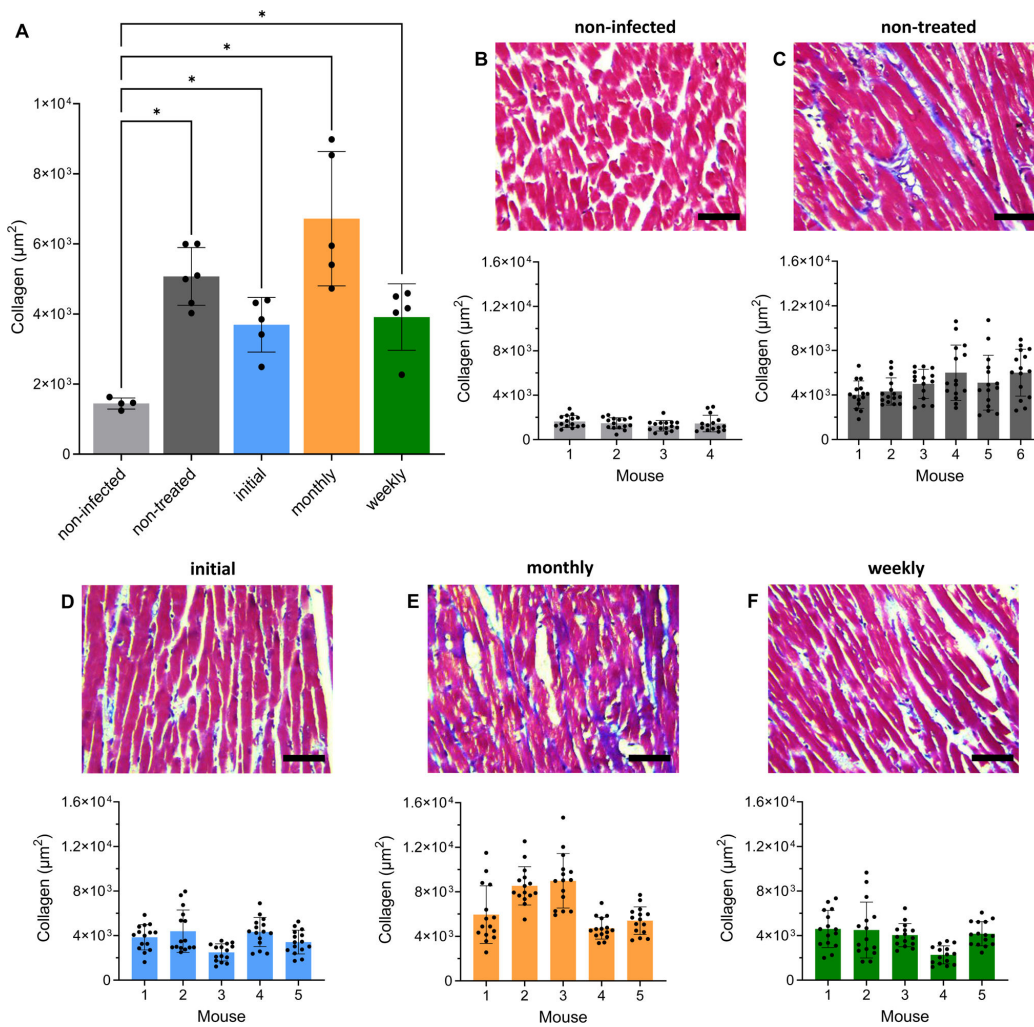


FIG 5 Intermittent posaconazole treatment does not protect *T. cruzi*-infected mice from cardiac pathology. (A) Bar chart showing collagen content (blue area in Masson's trichrome-stained sections) as a marker of cardiac fibrosis (Materials and Methods) in non-infected C3H/HeN mice ($n = 4$), mice infected with *T. cruzi* JR-Luc strain, non-treated ($n = 6$), and treated with posaconazole ($n = 5$ per treatment cohort). Each dot corresponds to a single mouse, with data expressed as mean \pm standard error of the mean (SEM). Asterisks represent P -values for one-way analysis of variance using Dunnett's multiple comparison *post-hoc* test ($*P < 0.05$), with a significant difference between the non-infected group and all infected groups. There was no significant difference ($P > 0.05$) between any of the treatment groups and the non-treated group. (B–F) Representative Masson's trichrome-stained photomicrographs highlighting collagen (blue) in cardiac sections from posaconazole-treated and non-treated mice. Magnification 400 \times , scale bars = 100 μ m. Bar charts show quantification of collagen content in individual mice from different groups, with each dot corresponding to the 15 randomly selected fields used for analysis and data expressed as mean \pm SEM.

sets in as mice progress through the chronic stage. Drug-induced functional restoration following curative treatment with benznidazole in the acute stage is associated with recovery of neuronal density in the myenteric plexus (32). In the current study, we also observed a biphasic curve in GI transit time during the course of non-treated infections (Fig. 4A). Non-curative suppressive treatment with posaconazole initiated during the acute stage (3 wpi) led to a rapid reversal of dysfunction, such that GI transit times returned to levels comparable with the non-infected control group. By week 12, however, the transit time in mice that had received only the initial posaconazole treatment returned to that in non-treated infected mice and then underwent further deterioration (Fig. 4A). Both the monthly and weekly intermittent treatment groups exhibited reversal

of the acute stage GI transit delay and also displayed a lag in the onset of the chronic stage symptoms. However, by week 24, gut motility subsequently declined to levels exhibited in non-treated mice (Fig. 4A and Fig. S2). By the end point, GI transit in the monthly and weekly intermittent treatment groups was significantly impaired in comparison with the non-infected group (Fig. S2). In benznidazole-cured mice, there is no deterioration in GI transit time during the chronic stage, indicating that a durable restoration of GI function is possible if a prompt sterile cure is achieved (32).

The partial improvement in GI transit times in non-treated mice toward the end of the acute stage, followed by further decline later in the chronic stage, suggests that two different mechanisms may be driving the GI transit pathology. This has parallels with CCC, where pathology in the acute stage is associated with myocarditis, and in the chronic stage, with cumulative damage and maladaptive fibrotic tissue repair that leads to cardiomyopathy (10). In the chronic stage, several mice in all the infected groups displayed GI transit time delays that were beyond the 4 h cut-off (Fig. 4A), indicating the development of more severe DCD pathology than observed earlier in the infection. *T. cruzi* infection of the GI tract leads to cumulative neuron loss in the enteric nervous system, resulting in a progressive decline in gut motility, particularly associated with the colon (31). To further investigate the functional deterioration of peristalsis, end-point assessment of fecal retention in the colon was also carried out. This constipation phenotype, similar to that in human DCD, revealed no significant improvement in mice that received non-curative treatment, compared to non-treated controls. All the treated groups showed a significant increase in fecal retention (Fig. 4B). Therefore, under the conditions tested, long-term suppressive posaconazole treatment does not lead to improvement in chronic DCD symptoms, as judged by GI transit delay or fecal retention.

In C3H/HeN mice chronically infected with the *T. cruzi* JR-Luc strain, the profile of organ/tissue parasite distribution is more disseminated than in other murine models, and up to 80% of mice display cardiac-localized infections when assessed by *ex vivo* imaging (23, 44). Mice display extensive cardiac fibrosis, a marker of CCC (22), irrespective of whether their hearts are infected at the point of analysis. Consistent with the DCD data, our results show that long-term non-curative intermittent posaconazole treatment also provides no significant protection against cardiac fibrosis at the experimental end-point (Fig. 5A). Therefore, despite suppression of the overall parasite burden, particularly with the weekly treatment regimen, there was no significant reduction in the severity of either GI tract or cardiac pathology. One possibility might be that the transient and fluctuating nature of recrudescence could impact the dynamics of the inflammatory immune response, such that this negates any beneficial outcome arising from a reduction in the overall parasite burden.

In summary, we have examined the impact of two intermittent posaconazole treatment regimens on three key aspects of chronic Chagas disease pathology (GI transit delay, fecal retention, and cardiac fibrosis). Our study demonstrates that these suppressive regimens do not prevent or alleviate long-term development of DCD or CCC, even when the parasite burden is considerably reduced. Although treatment with alternative regimens or therapeutics could reduce the parasite load further than described here, overall, these outcomes highlight that an ability to provide sterile cure should remain a pre-requisite of any anti-parasitic Chagas disease drug that is advanced to the clinic.

MATERIALS AND METHODS

Mouse husbandry, infections, and treatment

The *T. cruzi* JR strain (Discrete Typing Unit I; DTU I) modified to express the red-shifted luciferase gene, *PpyRE9h* (TcJR-Luc) (23, 52), was used in all experiments. Parasite growth and the generation of tissue culture trypomastigotes (TCTs) were as described previously (22). CB17-SCID mice purchased from Charles River (UK) were infected i.p. with 5×10^4 TCTs in 0.2 mL PBS and used to derive blood trypomastigotes (BTs) via cardiac puncture. Female C3H/HeN mice were also purchased from Charles River (UK) and infected, aged

7–10 weeks, with 1×10^3 BTs from SCID mice. Mice from each study group (Fig. 1) were housed in pathogen-free ventilated cages on a 12 h light/dark cycle with food and water *ad libitum*. Posaconazole (Biosynth, Ltd.; 20 mg/kg) was administered orally via gavage with a flexible cannula in a vehicle of 5% DMSO (v/v) and 95% (0.5% hydroxypropyl methylcellulose and 0.4% Tween 80 in Milli-Q H₂O). Non-treated mice were given vehicle only by oral gavage during the initial 12-day treatment period (Fig. 1). At the 31 week experimental end-point, all mice were euthanized by exsanguination under terminal anesthesia (dolethal, 60 mg/kg i.p.) and necropsied, with organs excised and imaged for bioluminescence. Specific organs were collected for further analysis (Fig. S1).

***In vivo* and *ex vivo* bioluminescence imaging**

All mice were injected with 150 mg/kg d-luciferin i.p. and anesthetized after 5 min using 2.5% (v/v) gaseous isoflurane in oxygen (52, 53). They were then imaged after a further 5 min using the IVIS Spectrum System (Revvity, Hopkinton, MA, USA), with anesthesia maintained through individual nose cones. Ventral and dorsal images were captured using Living Image v4.7.3, with exposure times of between 30 s and 5 min depending on signal intensity. The threshold for *in vivo* imaging was set at 5 min exposure, large binning, using non-infected mice. Mice were then revived and returned to their cages.

To estimate parasite load during the course of infection, regions of interest (ROIs) using Living Image v4.7.3 were drawn around *in vivo* images of individual mice captured during bioluminescence imaging (53, 54). This was expressed as total flux (photons/second). Estimated detection threshold values for *in vivo* imaging were attained using ROI data from non-infected mice on set imaging days throughout the study.

Mice were fasted for 2 h prior to necropsy for fecal pellet analysis. For *ex vivo* imaging, 150 mg/kg d-luciferin was i.p. injected, and mice were culled 5 min later by exsanguination under terminal anesthesia. The mice were perfused with 10 mL 0.3 mg/mL D-luciferin in PBS, and organs were excised and placed in a standardized arrangement on a Petri dish, along with the remaining carcass, and soaked in 0.3 mg/mL D-luciferin in PBS (53). Imaging of plated organs and carcass used 5 min exposure time and large binning.

Parasite recovery from mouse tissue

Excised organs were maintained in ice-cold Hanks' Balanced Salt Solution (HBSS) without calcium/magnesium until disaggregation. Tissues were minced into 3–4 mm pieces using sterile scalpels, washed 3× with PBS to remove blood/debris, transferred to a tube containing a freshly made collagenase solution (100 U/mL collagenase IV in HBSS), and incubated at 37°C for 2 h (55). The cell suspension was then filtered using a 200 µm cell strainer and centrifuged (300 g, 7 min). The pellet was resuspended in HBSS, and parasites were released using a 2 mL lysing matrix M (MP) in a Precellys 24 (Bertin) instrument, applying two cycles of 1 min at 5,000 speed. The suspension was then centrifuged (50 g, 5 min) to separate debris, and the supernatant was centrifuged (3,000 g, 5 min) to pellet the parasites. Parasites were then resuspended in epimastigote medium (56) and cultured in 48-well plates in a CO₂ incubator at 28°C.

***In vitro* posaconazole sensitivity assay**

To promote metacyclogenesis, TcJR-Luc epimastigotes were sub-cultured at 5×10^5 /mL and incubated for 14 days until stationary phase (~15% of the parasites transform). Next, 1–2 mL from the culture surface was transferred to an Eppendorf tube, and swimming metacyclic trypomastigotes were collected by centrifugation (3,000 g, 5 min). The pellet was resuspended in Minimum Essential Medium (MEM), supplemented with 5% heat-inactivated fetal bovine serum (FBS), 100 U/mL penicillin, and 100 µg/mL streptomycin, and added to a 60–70% confluent culture of COLO-N680 cells (a human esophageal squamous cell carcinoma line). This was maintained at 37°C in a CO₂ incubator with regular medium changes every 2–3 days. At day 8 post-infection, TCTs in the cell supernatant were collected by centrifugation, resuspended in Dulbecco's Modified Eagle Medium with high glucose (4 g/L), and counted.

Intrinsic luciferase expression in TcJR-Luc was used to monitor intracellular parasite replication. COLO-N680 cells (human esophageal squamous cell carcinoma line) were seeded at 5×10^4 cells per well in 100 μ L growth medium in white, clear-bottomed 96-well microplates. After 8 h, cells were infected overnight with 5×10^5 TCTs/well. The following day, wells were washed 3 \times with PBS to remove non-internalized TCTs before adding 200 μ L MEM supplemented with 2.5% FBS containing posaconazole at various concentrations. To assess activity, 8-point potency curves were generated by serial 2:1 dilution. At the experimental endpoint (96 h), wells were washed 1 \times with PBS and incubated for 30 min in 100 μ L fresh medium. Subsequently, 100 μ L reconstituted Bright-Glo Luciferase Assay System reagent (Promega) was added, and plates were incubated at room temperature for 2 min in the dark to allow cell lysis. Bioluminescence was quantified in triplicate using BMG FLUOstar Omega, with measurements obtained by integration over 3 s/well. Dose-response curves were fitted after calculating growth inhibition percentages compared to untreated controls for each clone. The 95% confidence intervals were calculated using the sigmoidal dose-response variable slope function in GraphPad Prism 10 software. Data are presented as the average of two independent experiments.

GI transit time assay

200 μ L 6% w/v Carmine red dye solution in 0.5% methyl cellulose mixed in distilled water was administered to individual mice by oral gavage. Mice were then returned to their cages for 75 min before being individually placed in separate containers. The time of the first red fecal pellet to be excreted was recorded. For animal welfare reasons, there was a maximum cut-off time of 4 h. Time from gavage to excretion of the first red pellet was recorded as the total intestinal transit time. For fecal pellet analysis, colons were separated from other tissues and externally cleaned with PBS. The fecal pellets were eased out of the colon lumen and counted (31, 32).

Histology and cardiac fibrosis

Mouse hearts were longitudinally bisected, placed in histology cassettes, and fixed with Glyo-fixx for 24 h at 4°C, then dehydrated in ethanol, cleared in xylene, and embedded in paraffin blocks at 56°C (53). Heart sections (5 μ m) were cut using a microtome, mounted on glass slides, dried overnight, and stained with Masson's trichrome. Quantification of collagen content was used as a marker for fibrosis, with 15 randomly selected fields per mouse used for analysis (17) and the investigator blinded to the groups. Using the binary processing prefilter function on the DFC420 light microscope (Leica Microsystems) and Leica Application Suite software v.4.2 for analysis, blue pixels were selected from the binary image for calculation of collagen fibers against the total area of cardiac muscle fibers staining red.

Statistics

The unit of analysis was classified as individual mice, with no blinding or randomization used. Statistical differences between groups were calculated using ordinary one-way analysis of variance with Dunnett's post-hoc correction for multiple comparisons from GraphPad Prism v.8, with differences of $P < 0.05$ considered significant.

ACKNOWLEDGMENTS

This work was supported by UK Medical Research Council (MRC) grants MR/T015969/1 to J.M.K. and MR/R021430/1 to M.D.L., and funding from the Drugs for Neglected Diseases initiative (DNDi). DNDi received financial support from Department for International Development (DFID), UK, Federal Ministry of Education and Research (BMBF) through KfW, Germany, and Médecins sans Frontières (MSF) International.

AUTHOR AFFILIATIONS

¹Department of Infection Biology, London School of Hygiene and Tropical Medicine, London, UK

²Department of Parasitology, Faculty of Sciences, University of Granada, Granada, Spain

PRESENT ADDRESS

Archie A. Khan, INSERM UMR 1235-TENS, The Enteric Nervous System in Gut and Brain Diseases, University of Nantes, Nantes, France

Michael D. Lewis, Division of Biomedical Sciences, Warwick Medical School, University of Warwick, Coventry, United Kingdom

AUTHOR ORCID*s*

Francisco Olmo  <http://orcid.org/0000-0001-9314-0026>

Amanda Fortes Francisco  <http://orcid.org/0000-0002-3475-8130>

John M. Kelly  <http://orcid.org/0000-0003-4305-5258>

FUNDING

Funder	Grant(s)	Author(s)
Medical Research Council		John M. Kelly
Medical Research Council	MR/R021430/1	Michael D. Lewis
Drugs for Neglected Diseases Initiative	NA	John M. Kelly

AUTHOR CONTRIBUTIONS

Shiromani Jayawardhana, Conceptualization, Data curation, Formal analysis, Investigation, Methodology, Writing – original draft, Writing – review and editing | Francisco Olmo, Data curation, Formal analysis, Investigation, Methodology, Supervision, Validation, Writing – review and editing | Amanda Fortes Francisco, Formal analysis, Investigation, Supervision, Validation, Visualization, Writing – review and editing | Archie A. Khan, Data curation, Formal analysis, Investigation, Methodology, Validation, Writing – review and editing | Michael D. Lewis, Funding acquisition, Methodology, Project administration, Supervision, Writing – review and editing | Martin C. Taylor, Conceptualization, Formal analysis, Supervision, Validation, Writing – review and editing | John M. Kelly, Conceptualization, Formal analysis, Funding acquisition, Project administration, Resources, Supervision, Writing – original draft

ETHICS APPROVAL

Animal studies were carried out under the UK Home Office licence P9AEE04E in accordance with the UK Animals (Scientific Procedures) Act 1986 and approved by the London School of Hygiene and Tropical Medicine Animal Welfare and Ethical Review Board.

ADDITIONAL FILES

The following material is available [online](#).

Supplemental Material

Supplemental material (AAC01786-24-S0001.pdf). Fig. S1 and S2.

REFERENCES

- World Health Organisation. 2023. Available from: [https://www.who.int/news-room/fact-sheets/detail/chagas-disease-\(american-trypanosomiasis\)](https://www.who.int/news-room/fact-sheets/detail/chagas-disease-(american-trypanosomiasis))
- Irish A, Whitman JD, Clark EH, Marcus R, Bern C. 2022. Updated estimates and mapping for prevalence of chagas disease among adults, United States. *Emerg Infect Dis* 28:1313–1320. <https://doi.org/10.3201/eid2807.212221>
- Gonzalez-Sanz M, Crespillo-Andújar C, Chamorro-Tojeiro S, Monge-Maillo B, Perez-Molina JA, Norman FF. 2023. Chagas disease in Europe. *Trop Med Infect Dis* 8:513. <https://doi.org/10.3390/tropicalmed8120513>
- De Fuentes-Vicente JA, Gutiérrez-Cabrera AE, Flores-Villegas AL, Lowenberger C, Benelli G, Salazar-Schettino PM, Córdoba-Aguilar A. 2018. What makes an effective Chagas disease vector? Factors underlying *Trypanosoma cruzi*-triatomine interactions. *Acta Trop* 183:23–31. <https://doi.org/10.1016/j.actatropica.2018.04.008>
- Edwards MS, Montgomery SP. 2021. Congenital Chagas disease: progress toward implementation of pregnancy-based screening. *Curr Opin Infect Dis* 34:538–545. <https://doi.org/10.1097/QCO.0000000000000769>
- Robertson LJ, Havelaar AH, Keddy KH, Devleeschauwer B, Sripa B, Torgerson PR. 2024. The importance of estimating the burden of disease from foodborne transmission of *Trypanosoma cruzi*. *PLoS Negl Trop Dis* 18:e0011898. <https://doi.org/10.1371/journal.pntd.0011898>
- Gómez LA, Gutierrez FRS, Peñuela OA. 2019. *Trypanosoma cruzi* infection in transfusion medicine. *Hematol Transfus Cell Ther* 41:262–267. <https://doi.org/10.1016/j.htct.2018.12.001>
- Rassi A Jr, Rassi A, Marin-Neto JA. 2010. Chagas disease. *Lancet* 375:1388–1402. [https://doi.org/10.1016/S0140-6736\(10\)60061-X](https://doi.org/10.1016/S0140-6736(10)60061-X)
- Pérez-Molina JA, Molina I. 2018. Chagas disease. *Lancet* 391:82–94. [https://doi.org/10.1016/S0140-6736\(17\)31612-4](https://doi.org/10.1016/S0140-6736(17)31612-4)
- Bonney KM, Luthringer DJ, Kim SA, Garg NJ, Engman DM. 2019. Pathology and pathogenesis of Chagas heart disease. *Annu Rev Pathol* 14:421–447. <https://doi.org/10.1146/annurev-pathol-020117-043711>
- Bonney KM, Engman DM. 2015. Autoimmune pathogenesis of Chagas heart disease: looking back, looking ahead. *Am J Pathol* 185:1537–1547. <https://doi.org/10.1016/j.ajpath.2014.12.023>
- Ribeiro AL, Nunes MP, Teixeira MM, Rocha MOC. 2012. Diagnosis and management of Chagas disease and cardiomyopathy. *Nat Rev Cardiol* 9:576–589. <https://doi.org/10.1038/nrcardio.2012.109>
- Cunha-Neto E, Chevillard C. 2014. Chagas disease cardiomyopathy: immunopathology and genetics. *Mediators Inflamm* 2014:683230. <https://doi.org/10.1155/2014/683230>
- Baldoni NR, de Oliveira-da Silva LC, Gonçalves ACO, Quintino ND, Ferreira AM, Bierrenbach AL, Padilha da Silva JL, Pereira Nunes MC, Ribeiro ALP, Oliveira CDL, Sabino EC, Cardoso CS. 2024. Gastrointestinal manifestations of Chagas disease: a systematic review with meta-analysis. *Am J Trop Med Hyg* 110:10–19. <https://doi.org/10.4269/ajtmh.23-0323>
- Dc-Rubin SSC, Schenkman S. 2012. *Trypanosoma cruzi* trans-sialidase as a multifunctional enzyme in Chagas' disease. *Cell Microbiol* 14:1522–1530. <https://doi.org/10.1111/j.1462-5822.2012.01831.x>
- Tarleton RL, Zhang L, Downs MO. 1997. "Autoimmune rejection" of neonatal heart transplants in experimental Chagas disease is a parasite-specific response to infected host tissue. *Proc Natl Acad Sci USA* 94:3932–3937. <https://doi.org/10.1073/pnas.94.8.3932>
- Francisco AF, Jayawardhana S, Taylor MC, Lewis MD, Kelly JM. 2018. Assessing the effectiveness of curative benznidazole treatment in preventing chronic cardiac pathology in experimental models of Chagas disease. *Antimicrob Agents Chemother* 62:e00832. <https://doi.org/10.1128/AAC.00832-18>
- Kierszenbaum F. 1999. Chagas' disease and the autoimmunity hypothesis. *Clin Microbiol Rev* 12:210–223. <https://doi.org/10.1128/CMR.12.2.210>
- Lewis MD, Kelly JM. 2016. Putting *Trypanosoma cruzi* dynamics at the heart of Chagas disease. *Trends Parasitol* 32:899–911. <https://doi.org/10.1016/j.pt.2016.08.009>
- Cutshaw MK, Sciaudone M, Bowman NM. 2023. Risk factors for progression to chronic Chagas cardiomyopathy: a systematic review and meta-analysis. *Am J Trop Med Hyg* 108:791–800. <https://doi.org/10.4269/ajtmh.22-0630>
- Roman-Campos D, Marin-Neto JA, Santos-Miranda A, Kong N, D'Ávila A, Rassi A Jr. 2024. Arrhythmogenic manifestations of Chagas disease: perspectives from the bench to bedside. *Circ Res* 134:1379–1397. <https://doi.org/10.1161/CIRCRESAHA.124.324507>
- Lewis MD, Fortes Francisco A, Taylor MC, Burrell-Saward H, McLatchie AP, Miles MA, Kelly JM. 2014. Bioluminescence imaging of chronic *Trypanosoma cruzi* infections reveals tissue-specific parasite dynamics and heart disease in the absence of locally persistent infection. *Cell Microbiol* 16:1285–1300. <https://doi.org/10.1111/cmi.12297>
- Lewis MD, Francisco AF, Taylor MC, Jayawardhana S, Kelly JM. 2016. Host and parasite genetics shape a link between *Trypanosoma cruzi* infection dynamics and chronic cardiomyopathy. *Cell Microbiol* 18:1429–1443. <https://doi.org/10.1111/cmi.12584>
- Ward AI, Lewis MD, Khan AA, McCann CJ, Francisco AF, Jayawardhana S, Taylor MC, Kelly JM. 2020. *In Vivo* analysis of *Trypanosoma cruzi* persistence *Foci* at single-cell resolution. *MBio* 11:e01242. <https://doi.org/10.1128/mBio.01242-20>
- Pérez-Mazliah D, Ward AI, Lewis MD. 2021. Host-parasite dynamics in Chagas disease from systemic to hyper-local scales. *Parasite Immunol* 43:e12786. <https://doi.org/10.1111/pim.12786>
- Porrello ER, Mahmoud AI, Simpson E, Hill JA, Richardson JA, Olson EN, Sadek HA. 2011. Transient regenerative potential of the neonatal mouse heart. *Science* 331:1078–1080. <https://doi.org/10.1126/science.1200708>
- Pinazo MJ, Cañas E, Elizalde JJ, García M, Gascón J, Gimeno F, Gomez J, Guhl F, Ortiz V, Posada EJ, Puente S, Rezende J, Salas J, Saravia J, Torrico F, Torrus D, Treviño B. 2010. Diagnosis, management and treatment of chronic Chagas' gastrointestinal disease in areas where *Trypanosoma cruzi* infection is not endemic. *Gastroenterol Hepatol* 33:191–200. <https://doi.org/10.1016/j.gastrohep.2009.07.009>
- Dantas RO. 2021. Management of esophageal dysphagia in Chagas disease. *Dysphagia* 36:517–522. <https://doi.org/10.1007/s00455-021-10297-1>
- de Oliveira RB, Troncon LE, Dantas RO, Menghelli UG. 1998. Gastrointestinal manifestations of Chagas' disease. *Am J Gastroenterol* 93:884–889. https://doi.org/10.1111/j.1572-0241.1998.270_r.x
- Arantes RME, Marche HFF, Bahia MT, Cunha FQ, Rossi MA, Silva JS. 2004. Interferon-gamma-induced nitric oxide causes intrinsic intestinal denervation in *Trypanosoma cruzi*-infected mice. *Am J Pathol* 164:1361–1368. [https://doi.org/10.1016/s0002-9440\(10\)63222-1](https://doi.org/10.1016/s0002-9440(10)63222-1)
- Khan AA, Langston HC, Costa F, Olmo F, Taylor MC, McCann CJ, Kelly JM, Lewis MD. 2021. Local association of *Trypanosoma cruzi* chronic infection foci and enteric neuropathic lesions at the tissue micro-domain scale. *PLoS Pathog* 17:e1009864. <https://doi.org/10.1371/journal.ppat.1009864>
- Khan AA, Langston HC, Walsh L, Roscoe R, Jayawardhana S, Francisco AF, Taylor MC, McCann CJ, Kelly JM, Lewis MD. 2024. Enteric nervous system regeneration and functional cure of experimental digestive Chagas disease with trypanocidal chemotherapy. *Nat Commun* 15:4400. <https://doi.org/10.1038/s41467-024-48749-5>
- Wilkinson SR, Kelly JM. 2009. Trypanocidal drugs: mechanisms, resistance and new targets. *Expert Rev Mol Med* 11:1–24. <https://doi.org/10.1017/S1462399409001252>
- Lascano F, García Bournissen F, Altchek J. 2022. Review of pharmacological options for the treatment of Chagas disease. *Br J Clin Pharmacol* 88:383–402. <https://doi.org/10.1111/bcp.14700>
- Molina I, Gómez Prat J, Salvador F, Treviño B, Sulleiro E, Serre N, Pou D, Roure S, Cabezos J, Valerio L, Blanco-Grau A, Sánchez-Montalvá A, Vidal X, Pahissa A. 2014. Randomized trial of posaconazole and benznidazole for chronic Chagas' disease. *N Engl J Med* 370:1899–1908. <https://doi.org/10.1056/NEJMoa1313122>
- Morillo CA, Marin-Neto JA, Avezum A, Sosa-Estani S, Rassi A Jr, Rosas F, Villena E, Quiroz R, Bonilla R, Britto C, Guhl F, Velazquez E, Bonilla L, Meeks B, Rao-Melacini P, Pogue J, Mattos A, Lazdins J, Rassi A, Connolly SJ, Yusuf S, BENEFIT Investigators. 2015. Randomized trial of benznidazole for chronic Chagas' cardiomyopathy. *N Engl J Med* 373:1295–1306. <https://doi.org/10.1056/NEJMoa1507574>
- Wilkinson SR, Taylor MC, Horn D, Kelly JM, Cheeseman I. 2008. A mechanism for cross-resistance to nifurtimox and benznidazole in trypanosomes. *Proc Natl Acad Sci USA* 105:5022–5027. <https://doi.org/10.1073/pnas.0711014105>
- Mejia AM, Hall BS, Taylor MC, Gómez-Palacio A, Wilkinson SR, Triana-Chávez O, Kelly JM. 2012. Benznidazole-resistance in *Trypanosoma cruzi* is a readily acquired trait that can arise independently in a single

- population. *J Infect Dis* 206:220–228. <https://doi.org/10.1093/infdis/jis331>
39. Urbina JA. 2009. Ergosterol biosynthesis and drug development for Chagas disease. *Mem Inst Oswaldo Cruz* 104:311–318. <https://doi.org/10.1590/s0074-02762009000900041>
40. Lepesheva GI, Villalta F, Waterman MR. 2011. Targeting *Trypanosoma cruzi* sterol 14 α -demethylase (CYP51). *Adv Parasitol* 75:65–87. <https://doi.org/10.1016/B978-0-12-385863-4.00004-6>
41. Raad II, Graybill JR, Bustamante AB, Cornely OA, Gaona-Flores V, Afif C, Graham DR, Greenberg RN, Hadley S, Langston A, Negrón R, Perfect JR, Pitisuttithum P, Restrepo A, Schiller G, Pedicone L, Ullmann AJ. 2006. Safety of long-term oral posaconazole use in the treatment of refractory invasive fungal infections. *Clin Infect Dis* 42:1726–1734. <https://doi.org/10.1086/504328>
42. Wong TY, Loo YS, Veetil SK, Wong PS, Divya G, Ching SM, Menon RK. 2020. Efficacy and safety of posaconazole for the prevention of invasive fungal infections in immunocompromised patients: a systematic review with meta-analysis and trial sequential analysis. *Sci Rep* 10:14575. <https://doi.org/10.1038/s41598-020-71571-0>
43. Morillo CA, Waskin H, Sosa-Estani S, Del Carmen Bangher M, Cuneo C, Milesi R, Mallagray M, Apt W, Beloscar J, Gascon J, Molina I, Echeverria LE, Colombo H, Perez-Molina JA, Wyss F, Meeks B, Bonilla LR, Gao P, Wei B, McCarthy M, Yusuf S, STOP-CHAGAS Investigators. 2017. Benznidazole and posaconazole in eliminating parasites in asymptomatic *T. Cruzi* carriers: the STOP-CHAGAS trial. *J Am Coll Cardiol* 69:939–947. <https://doi.org/10.1016/j.jacc.2016.12.023>
44. Francisco AF, Lewis MD, Jayawardhana S, Taylor MC, Chatelain E, Kelly JM. 2015. Limited ability of posaconazole to cure both acute and chronic *Trypanosoma cruzi* infections revealed by highly sensitive *in vivo* imaging. *Antimicrob Agents Chemother* 59:4653–4661. <https://doi.org/10.1128/AAC.00520-15>
45. Santos FM, Mazzeti AL, Caldas S, Gonçalves KR, Lima WG, Torres RM, Bahia MT. 2016. Chagas cardiomyopathy: the potential effect of benznidazole treatment on diastolic dysfunction and cardiac damage in dogs chronically infected with *Trypanosoma cruzi*. *Acta Trop* 161:44–54. <https://doi.org/10.1016/j.actatropica.2016.05.007>
46. Calvet CM, Choi JY, Thomas D, Suzuki B, Hirata K, Lostracco-Johnson S, de Mesquita LB, Nogueira A, Meuser-Batista M, Silva TA, Siqueira-Neto JL, Roush WR, de Souza Pereira MC, McKerrow JH, Podust LM. 2017. 4-aminopyridyl-based lead compounds targeting CYP51 prevent spontaneous parasite relapse in a chronic model and improve cardiac pathology in an acute model of *Trypanosoma cruzi* infection. *PLoS Negl Trop Dis* 11:e0006132. <https://doi.org/10.1371/journal.pntd.0006132>
47. Drugs for Neglected Diseases Initiative. 2024. Available from: <https://dndi.org/diseases/chagas/>
48. Francisco AF, Jayawardhana S, Olmo F, Lewis MD, Wilkinson SR, Taylor MC, Kelly JM. 2020. Challenges in Chagas disease drug development. *Molecules* 25:2799. <https://doi.org/10.3390/molecules25122799>
49. Olmo F, Jayawardhana S, Khan AA, Langston HC, Francisco AF, Atherton RL, Ward AI, Taylor MC, Kelly JM, Lewis MD. 2024. A panel of phenotypically and genotypically diverse bioluminescent fluorescent *Trypanosoma cruzi* strains as a resource for Chagas disease research. *PLoS Negl Trop Dis* 18:e0012106. <https://doi.org/10.1371/journal.pntd.0012106>
50. Francisco AF, Sousa GR, Vaughan M, Langston H, Khan A, Jayawardhana S, Taylor MC, Lewis MD, Kelly JM. 2023. Cardiac abnormalities in a predictive mouse model of Chagas disease. *Pathogens* 12:1364. <https://doi.org/10.3390/pathogens12111364>
51. Moraes CB, Giardini MA, Kim H, Franco CH, Araujo-Junior AM, Schenkman S, Chatelain E, Freitas-Junior LH. 2014. Nitroheterocyclic compounds are more efficacious than CYP51 inhibitors against *Trypanosoma cruzi*: implications for Chagas disease drug discovery and development. *Sci Rep* 4:4703. <https://doi.org/10.1038/srep04703>
52. Branchini BR, Ablamsky DM, Davis AL, Southworth TL, Butler B, Fan F, Jathoul AP, Pule MA. 2010. Red-emitting luciferases for bioluminescence reporter and imaging applications. *Anal Biochem* 396:290–297. <https://doi.org/10.1016/j.ab.2009.09.009>
53. Taylor MC, Francisco AF, Jayawardhana S, Mann GS, Ward A, Olmo F, Lewis MD, Kelly JM. 2019. Exploiting genetically modified dual-reporter strains to monitor experimental *Trypanosoma cruzi* infections and host:parasite interactions *T. cruzi* infection: methods and protocols. Edited by KA Gomez and CA Buscaglia. *Methods Molec Biol* 1955:147–163. https://doi.org/10.1007/978-1-4939-9148-8_11
54. Lewis MD, Francisco AF, Taylor MC, Kelly JM. 2015. A new experimental model for assessing drug efficacy against *Trypanosoma cruzi* infection based on highly sensitive *in vivo* imaging. *J Biomol Screen* 20:36–43. <https://doi.org/10.1177/1087057114552623>
55. Freshney R. 1987. Culture of animal cells: a manual of basic techniques, p 117. Alan R Liss Inc, New York.
56. Kendall G, Wilderspin AF, Ashall F, Miles MA, Kelly JM. 1990. *Trypanosoma cruzi* glycosomal glyceraldehyde-3-phosphate dehydrogenase does not conform to the “hotspot” topogenic signal model. *EMBO J* 9:2751–2758. <https://doi.org/10.1002/j.1460-2075.1990.tb07462.x>